Journal of Medicinal and Aromatic Plant Sciences 43(3-4), 2021, 108-116

ORIGINAL RESEARCH ARTICLE

Dactyloidin from *Myristica fatua* Houtt. seed enhances glucose uptake through translocation of GLUT4 *via* upregulation of AMPK in L6 myotubes

PRABHA B[1] • SINI S[2] • SHERIN DR[3] • NEETHU S[1,4] • GOVIND MG[5] • DAN M[6,*] MANOJKUMAR TK[3,*] • JAYAMURTHY P[2,4,*] • RADHAKRISHNAN KV[4,*]

Article History

Received: June 12th, 2021
Revised: September 18th, 2021
Accepted: October 12th, 2021

Key Words

AMPK pathway
Dactyloidin
Glucose uptake
GLUT4 translocation
Human maltase glucoamylase
α-glucosidase inhibition

ABSTRACT

*Dactyloidin (DTN), a diarylnonanoid, was isolated for the first time from the seeds of Myristica fatua Houtt. DTN displayed significant inhibitory activity on α-glucosidase enzyme with IC_{50} value of 55.08 ± 0.857 μM. Molecular docking studies showed that DTN effectively binds to the active sites of N- terminal human maltase glucoamylase (**3TOP**), which supported the observed α-glucosidase inhibition. DTN also exhibited an enhanced glucose uptake in L6 myotubes with 31.5%. Exhilarated with these observations, we investigated the molecular mechanism of DTN by investigating the modulation of AMPK. The results revealed that DTN increased the glucose uptake in L6 myotubes by stimulating the translocation and expression of GLUT4.*

INTRODUCTION

Type 2 diabetes mellitus (T2DM) is one of the most widespread metabolic syndromes, characterized by hyperglycemia because of the abnormalities of insulin production and its usage (DeFronzo *et al.*, 2015). Inhibition of digestive enzymes, delaying of advanced glycated end products (AGEs) formation, and glucose uptake in myocytes and adipocytes are the well-studied method for controlling blood glucose levels and the associated diabetic complications (Trapero *et al.*, 2012; Prabhakar *et al.*, 2011). GLUT4 plays a major role in enhancing the transport of glucose in tissues. Thus increasing GLUT4 expression in skeletal muscle and adipose tissue could be an effective therapy for the treatment of insulin resistance and T2DM (Huang & Czech, 2007). Further more, 52-adenosine-monophosphate-activated protein kinase (AMPK) in insulin-independent glucose uptake and GLUT4 is under the regulation of AMPK, which supports the cellular energy homeostasis the activation of AMPK results in phosphorylation, which enhances the uptake of glucose in skeletal muscles. Hence, AMPK is an attractive therapeutic target for the treatment of T2DM (Kim & Park, 2016). The existing diabetic medications, including insulin injections and hypoglycemic drugs, are effective to the patients but have many drawbacks, including limited efficacy, weight gain, hypoglycemic risk and hepatotoxicity (Victor & John, 2006). To overcome these challenges, we focused on the development of potent antidiabetic agents from natural cradles.

*Corresponding author; Email: radhu2005@gmail.com
[1]Chemical Sciences and Technology Division, CSIR-National Institute for Interdisciplinary Science and Technology, Thiruvananthapuram-695019, India, [2]Agroprocessing and Technology Division, CSIR-National Institute for Interdisciplinary Science and Technology, Thiruvananthapuram-695019, India, [3]School of Digital Sciences, Kerala University of Digital Sciences Innovation and Technology, Thiruvananthapuram-695 317, India, [4]Academy of Scientific and Innovative Research (AcSIR), Thiruvananthapuram-695019, India [5]Plant Genetics Resource Division, Jawaharlal Nehru Tropical Botanic Garden and Research Institute, Palode, Thiruvananthapuram-695562, India.
Doi: https://doi.org/10.62029/jmaps.v43i3.Prabha

Myristica fatua Houtt. var. *Magnifica* (Bedd.) Sinclair (*M. fatua*) belongs to the Myristicaceae family, commonly known as wild nutmeg, endemic to freshwater swamps of southern Western Ghats, India. Recent studies have shown that acyl phenols and lignans are the major class of phytochemicals present in this species, and they exhibit antiproliferative, antimicrobial, antimycobacterial and antidiabetic activities (Pandey *et al.*, 2016; Fajriah *et al.*, 2017; Megawati & Darmawan, 2017; Prabha *et al.*, 2018; Prabha *et al.*, 2019; Herath *et al.*, 1998). We described herein the isolation, characterization and antidiabetic potential of a diarylnonanoid, dactyloidin (DTN) from the seeds of *M. fatua*.

MATERIALS AND METHODS

General experimental procedures and chemicals used

The melting point was measured using Buchi melting point apparatus and IR spectrum with a Bruker FT-IR spectrometer. 1D and 2D NMR spectra were recorded on a Bruker Avance 500 MHz spectrometer. HRESIMS was acquired on a Thermo Scientific Exactive mass spectrometer. Column chromatography was performed using silica gel (100-200 mesh; Merck, Darmstadt, Germany) and Merck precoated silica gel F_{254} plates were used for monitoring thin-layer chromatography (TLC). Spots were visualized under UV light (254 and 365 nm) and by spraying with a *p*-anisaldehyde-sulfuric acid solution followed by heating.

Porcine pancreatic α-amylase, α-glucosidase from *Saccharomyces cerevisiae*, acarbose, bovine serum albumin (BSA), α-D-glucose, ascorbic acid, metformin, 4-nitrophenyl α-D-glucopyranoside (*p*-NPG), Dulbecco's modified Eagle's media (DMEM), fetal bovine serum (FBS), antibiotic-antimycotic solution (Pencillin–streptomycin–amphotericin B mix) and 3-(4,5-dimethylthiazol-2-yl)-2,5-diphenyl tetrazolium bromide (MTT), were purchased from M/s Sigma–Aldrich Chemicals (St. Louis, MO, USA). 2-(N-(7-nitrobenz-2-oxa-1, 3-diazol-4-yl) amino)-2-deoxyglucose (2-NBDG) was procured from a molecular probe (Invitrogen Life Technologies, Carlsbad, CA, USA). Phospho-specific or pan-specific antibodies against AMPK, and GLUT 4 were procured from Santa Cruz Biotechnology, USA.

Plant material

Seeds of *Myristica fatua* Houtt. var. *Magnifica* (Bedd.) Sinclair were collected at Agasthyamalai Biosphere Reserve of South Western Ghats region of Kollam District, Kerala, India in December 2016 and identified by the plant taxonomist of Jawaharlal Nehru Tropical Botanic Garden and Research Institute, India. A voucher specimen (**TBGT 83441**) was deposited at the herbarium of the repository of the same institute.

Extraction, isolation and characterization of secondary metabolite

The dried and milled seeds of *M. fatua* (850 g) were extracted with DCM at room temperature. The solvent was removed under reduced pressure to give 60 g of crude DCM extract. The extract (60 g) was fractionated by silica gel CC using hexane, EtOAc, and MeOH as eluent to give 18 fractions based on TLC analysis. Fraction 13 and 14 was subjected to CC separation using EtOAc/hexane as eluent, which afforded dactyloidin as a colourless crystal (35 mg).

α-Amylase inhibitory activity

The porcine pancreatic α-amylase inhibitory activity was determined using the method described by Xio *et al.* with slight modification (Xio *et al.*, 2006). Different concentrations of DTN (10 µM, 20 µM, 30 µM, 40 µM, and 50 µM) were added to the reaction mixture containing sodium phosphate buffer (0.1 M), 40 µL of porcine pancreatic α-amylase (1 UmL^{-1}) and 40 µL of soluble starch (2.8 mg/mL). The reaction mixture was then incubated at 50 °C for 30 min. Then, the reaction was terminated by adding 1 M HCl, followed by the addition of 100 µL of iodine reagent (0.05 M). The absorbance was read at 580 nm on a microplate reader (Synergy 4 Biotek multiplate reader, USA). Here, acarbose was used as the standard. The percentage of inhibition was calculated using the following equation,

$$\% \text{ of inhibition} = \frac{\text{The absorbance of control - Absorbance of sample}}{\text{Absorbance of control}} \times 100$$

α-Glucosidase inhibitory activity

The *a*-glucosidase inhibitory effect of DTN was assayed according to the procedure described previously by Adisakwattana *et al.* with minor

modifications (Apostolidis *et al.*, 2007). Different concentrations of DTN (20 µM, 40 µM, 60 µM, 80 µM, and 100 µM) containing 10 µLof α-glucosidase solutions (1.0 UmL^{-1}) were mixed and kept at room temperature for 5 min. Then, 250 µL of *p*-NPG (7 mM) was added and incubated at 37 °C for 20 min. After incubation time, Na_2CO_3 solution (0.2 M) was added to terminate the reaction. The standard drug, acarbose, was used as a positive control. The enzymatic activity was calculated by assessing the *p*-nitrophenol released from *p*-NPG at 405 nm wavelength, and the percentage inhibition was calculated using the above equation.

Antiglycation property

Antiglycation property was analyzed as depicted by Jedsadayanmata with slight modifications (Jedsadayanmata 2005). The BSA was incubated with 500 mM of α-D-glucose along with different concentrations of the DTN (100 µM, 200 µM, 300 µM, 400 µM, and 500 µM) in 0.2 M potassium phosphate-buffered saline at 60 °C for 24 h. The reaction was stopped by adding 100% trichloroacetic acid (TCA) and kept at 4 °C for 10 min. Further, the samples were centrifuged (10,000 g), and the precipitate was dissolved in alkaline PBS. The fluorescence of the advanced glycated end products (AGEs) was measured using excitation at 370 nm, and emission at 440 nm and the AGEs formation was calculated using the following equation,

$$\text{AGEs formation} = \frac{\text{Fluorescence of control - Fluorescence of sample}}{\text{Fluorescence of control}} \times 100$$

In silico studies

The crystallized structures of target proteins human pancreatic α-amylase (PDB code: **4GQQ**) (Williams *et al.,* 2012) and *C*-terminal and *N*-terminal of human maltase-glucoamylase (PDB code: **3TOP and 2QMJ**) (Ren *et al.,* 2011; Sim *et al.,* 2008) were retrieved from RCSB Protein Data Bank (PDB). The α-amylase structure consists of a polypeptide chain with 496 amino acids, and the resolution of the structure was 1.35 Å, whereas in the case of the human maltase-glucoamylase the resolution of the structures is 2.8 and 1.9 Å, which consists of polypeptide chains of lengths 908 and 870 amino acids respectively. These proteins were prepared for docking by Protein Preparation Wizard of Schrodinger suite 2017-2. The grid was generated in the binding sites assumed around the centroid of the workspace ligand. The prepared proteins were then docked against the different conformers of the ligand DTN generated by the ligprep tool, using glide-ligand docking of the Schrodinger suite. The docked poses were then ranked based on Dock score (D-score) and Glide score (G-score) values. The absorption, distribution, metabolism and excretion/toxicity (ADME/T) were predicted based on the values for pharmacokinetic parameters available from qikprop.

Cell culture and treatment conditions

L6 myocytes were procured from NCCS, Pune, India and were maintained in DMEM containing 10% FBS and 1% antibiotic–antimycotic mix at 37 °C in humidified air containing 5% CO_2. For differentiation, the cells were maintained in differentiation media containing 2% horse serum for 5-7 days, and the medium was replaced every 2 days.

Cytotoxicity assay

Cytotoxicity was assessed using MTT assay (Mosmann 1983). The cells were maintained at 37° C in 5% CO_2 incubator. They were trypsinized and seeded in 24 well plates ($1x10^4$ cells per well) and attaining the confluency, treated with different concentrations of the DTN (2.5 µM, 5 µM, 10 µM, 25 µM, 50 µM and 100 µM) for 24 h. After the incubation, cells were treated with MTT reagent (0.5 g/L) for 4 hours. Mitochondrial dehydrogenase enzyme is active only in live cells that reduce the yellow dye, MTT, to purple formazan crystals, and the crystals were dissolved in 200 µL DMSO. The absorbance was recorded at 570 nm using a Synergy 4 Biotek multimode reader. The percentage of cell toxicity was calculated as,

$$\% \text{ of cell toxicity} = \frac{\text{The absorbance of control - Absorbance of}}{\text{Absorbance of control}} \times 100$$

Fluorescence analysis of 2-NBDG uptake by flow cytometry

Glucose uptake of active concentration of DTN was confirmed by flow cytometry analysis (Somwar *et al.*, 1998; Tamrakar *et al.*, 2011). Briefly, after differentiation for 5 days, cells were pre-treated with 2.5 µM concentration of DTN for 24 h. After

removal of the culture medium, the cells were washed two times with precooled PBS. The cells were then treated with the fluorescent analogue of glucose, 2- NBDG (10 mM) and incubated for 30 min. The uptake of 2-NBDG by the cells was stopped by removing the incubation medium, and the cells were washed twice with precooled PBS. Cells were then trypsinized and resuspended in ice-cold PBS, and subjected to flow cytometry. Samples were analyzed using BD FACS Aria II (BD Biosciences) at the FITC range (excitation 490 nm, emission 525 nm bandpass filter). The mean fluorescence intensity of different groups was analyzed by BD FACS Diva software and corrected for autofluorescence from unlabelled cells. Here, the standard drug, metformin (100 µM), served as a positive control.

Western blot for the expression of AMPK and GLUT4 in L6 myotubes

The expression level of GLUT 4 and AMPK protein was evaluated by Western blotting (Burnette, 1981). L6 myotubes were treated with 2.5 µM of DTN for 24 h. After incubation, the cells were lysed in ice-cold lysis buffer (50 mM Tris-HCl, 150 mM sodium chloride, 1.0% Igepal CA-630, 0.5% sodium deoxycholate, 0.1% sodium dodecyl sulfate, 1% Triton X-100 and protease inhibitor cocktail, pH 8.0) for 30 min on ice and were centrifuged at 12000 xg for 10 min. The protein content was then measured using BCA protein assay kit. The lysates (40 µg) were subjected to SDS-PAGE on 10% gel and transferred on to a polyvinylidene difluoride (PVDF, Immobilon P™, Millipore®, USA) membrane by using Trans-Blot Turbo™ (Bio-Rad). The membranes were blocked by incubating in blocking buffer (5% skim milk in PBST, PBST-PBS buffer containing 0.1% Tween 20) for 1 h at room temperature, washed three times with PBST and probed over night at 4° C with appropriate antibody against AMPK and GLUT4 (1: 1000). Membranes were washed 3 times and incubated for 1h at room temperature with horse radish peroxidase (HRP) conjugated secondary antibody at 1:1000 dilution and again washed three times in PBST. The bound antibodies were detected using an enhanced chemiluminescence substrate (Biorad, USA) and measured by densitometry using a Chemi Doc XRS digital imaging system and the Multi Analyst software from Bio-Rad Laboratories (USA).

Statistical analysis

All statistical analysis was performed with GraphPad Prism Software (San Diego, CA). After confirming a Gaussian distribution of the results, the comparison was made using the Students unpaired t-test. Data are presented as mean ± SD; p-values <0.05 were considered as significant.

RESULTS AND DISCUSSIONS

Isolation and characterization

The dichloromethane extract of the dried and ground seeds of *M. fatua* was subjected to separation and purification led to the isolation of a diarylnonanoid, dactyloidin (DTN). Structure and single crystal X-ray (CCDC 1839013) of the DTN are shown in **Figure 1**, and the NMR and HRESIMS spectrum of DTN is depicted in the supplementary information (Figure S1-S7).

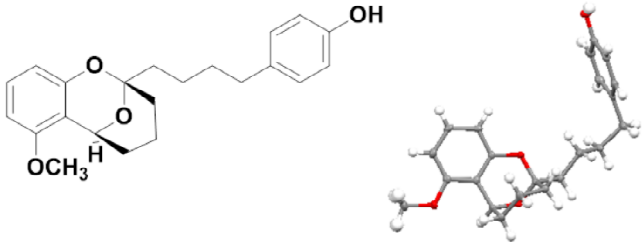

Figure 1: Structure and single crystal X-Ray of dactyloidin

DTN was obtained as white crystalline solid. Its HRESIMS spectrum showed the $[M+Na]^+$ ion at m/z 377.17260 leading to the molecular formula $C_{22}H_{26}O_4$. ^{1}H NMR (500 MHz, Acetone-d_6): 8.08 (s, 1H), 7.10 (t, *J* = 8 & 8.5 Hz, 1H), 7.03 (d, *J* = 8.5 Hz, 2H), 6.75 (d, *J* = 8.5 Hz, 2H), 6.47 (d, *J* = 8 Hz, 1H), 6.41 (d, *J* = 8 Hz, 1H), 5.15 (d, *J* = 3.5 Hz, 1H), 3.81 (s, 3H), 2.53 (t, *J* = 7 and 8 Hz, 2H), 1.96 (m, 1H), 1.87 (brd, *J* = 13.5 Hz, 1H), 1.74 (m, 3H), 1.70 (m, 1H), 1.62-1.55 (m, 4 H), 1.53-1.49 (m, 2H) ppm. ^{13}C NMR (125 MHz, Acetone-d_6): ä 155.4, 155.2, 154.9, 133.2, 129.2, 128.0, 115.0, 111.4, 107.6, 101.4, 99.8, 66.6, 55.0, 40.8, 34.8, 34.7, 31.9, 29.4, 21.9, 15.8 ppm (Herath *et al.*, 1998).

In vitro and *in silico* studies of DTN on digestive enzymes

The digestive enzymes, *i.e.*, α-amylase and α-glucosidase, act as dual inhibitor that slows down the release of glucose from oligosaccharides, thus delaying glucose absorption and decreasing

postprandial blood glucose levels. As part of our continuing research to identify promising digestive enzyme inhibitors from natural products and synthetically modified natural products(Ajish *et al.*, 2015; Sasikumar *et al.*, 2016; Sasikumar *et al.*, 2018; Sasikumar *et al.*, 2019; Gopalan *et al.*, 2019; Gopalan *et al.*, 2017; Dhanya *et al.*, 2017) herein we focused digestive enzyme inhibitory activity of DTN. DTN exhibited inhibitory activity on α-amylase with IC_{50} value of 32.55±0.833 µM, whereas the positive control, acarbose, showed an IC_{50} value of 8.234±1.784 µM ($p < 0.01$). The DTN displayed significant α-glucosidase inhibitory activity with an IC_{50} value of 55.08±0.857 µM ($p < 0.01$). The standard α-glucosidase inhibitor, acarbose, exhibited IC_{50} value of 52.04 ± 872 µM ($p < 0.01$). Exhilarated with these results, we analyzed the interaction of DTN with human pancreatic α-amylase (**4GQQ**) and human maltase glucoamylase (*N*- terminal; **3TOP** & *C*-terminal; **2QMJ**) by molecular docking techniques.

The proteins from PDB were refined, minimized, optimized, and their grids were generated. The protein with the grid defined around the pocket was further used for docking with the different conformers of the ligand, DTN under study. Qikprop analysis predicts the ADME/T properties. These are well suited for a drug as per pharmacokinetic parameters (Table 1). The ligand is more drug-like with a #stars value of 0, central nervous system toxicity 0, % human oral absorption maximum and with minimum deviation from Lipinski rule of 5. The D-score and G-score values interpret the stability of the ligands in the binding site and also strengthen the druggability of the ligands (Figure 2). In all the three binding pockets, DTN showed appreciable D-scores and G-scores. The affinity is greatest for **3TOP** with a D-score and G-score of -5.7. The phenolic -OH of DTN form strong H-bond with Asp 236 and –O with Ser 245 of 4GQQ. While in **3TOP** and **2QMJ**, the phenolic -OH forms H-bonds with Asp 203 and Arg 202, and there are π-stacking interactions of the two terminal benzene rings with Lys 480 and Phe 575. The 2D and 3D interaction diagrams of DTN with 4GQQ, 2QMJ and 3TOP are shown in Figure 2.

M.W. (Molecular Weight): 130.0 to 725.0; #stars (few stars-more drug-like): 0 to 5; #rotor (Number of non-trivial and non-hindered rotatable bonds):

Table 1: ADME/T properties of Dactyloidin

Sl. No	Dactyloidin
M.W	354.445
#stars	0
#rotor	7
CNS	0
SASA	665.093
FISA	54.673
HBA	3
HBD	1
QPlogKhsa	0.947
HOA	3
% HOA	100
QPlogPo/w	5.338
QPlogS	-6.16
R Of Five	1

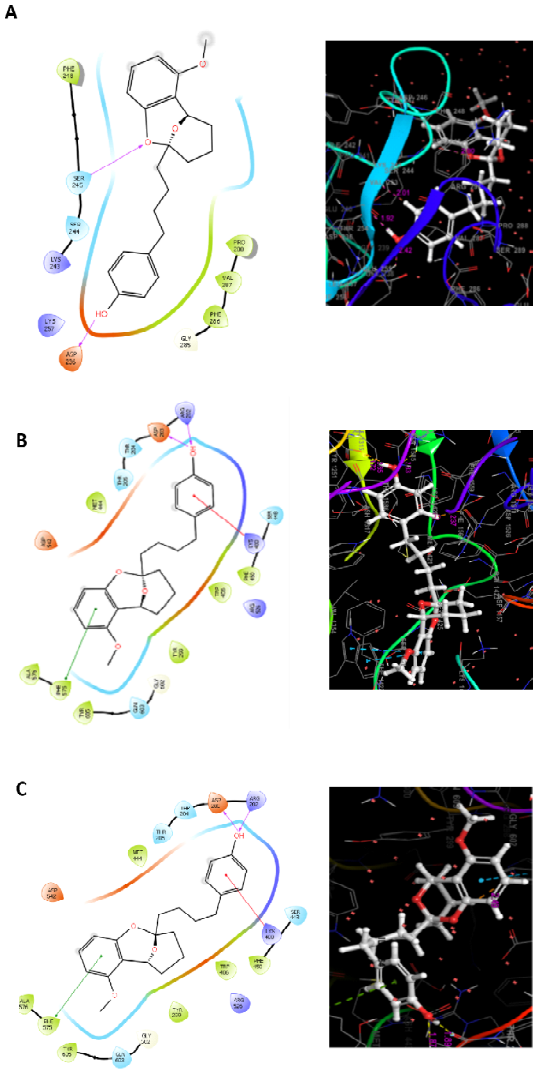

Figure 2: Two-and three-dimensional interaction diagrams of dactyloidin with (A) 4GQQ, (B) 2QMJ and (C) 3TOP.

0 to 15; CNS (Central Nervous System activity): -2 to +2; SASA (Total solvent accessible surface area in square angstroms): 300.0 to 1000.0 FISA (Hydrophilic component of total solvent accessable area): 7.0 to 333.0; HBA (Hydrogen bond acceptor): 2.0 to 20.0; HBD (hydrogen bond donor): 0.0 to 6.0; QPlogKhsa (binding to human serum albumin): -1.5 to 1.5; HOA (Human Oral Absorption): 1, 2, or 3 for low medium, and high; % HOA (Percent Human Oral Absorption): >80 % is high, <25 % is poor; QPlogPo/w (octanol/water partition coefficient): -2.0 to 6.5; QPlogS (Aqueous solubility): -6.5 to 0.5; Ro5 (Number of violations of Lipinski's rule of five): maximum is 4.

Protein glycation property

In the hyperglycemic condition, excess glucose reacts with proteins to form advanced glycated end products (AGEs), which further causes diabetic associated complications (Adrover *et al.*, 2014).[21] In this aspect, we have evaluated the effect on the glycation process, and the result indicated that DTN inhibited *in vitro* glycation with IC_{50} value of 262.73±0.577 µM ($p < 0.01$). Here, we used ascorbic acid as a positive control which showed an IC_{50} value of 155.38 ± 0.547 µM ($p < 0.01$).

Cell toxicity

Cytotoxicity was performed in L6 myocytes using MTT assay with 2.5 µM to 100 µM concentration of DTN. DTN treatment at a concentration up to 2.5 µM for 24 hr has shown any sign of cytotoxicity. Therefore, 2.5 µM concentration was chosen for further cell-based experiments (Figure 3).

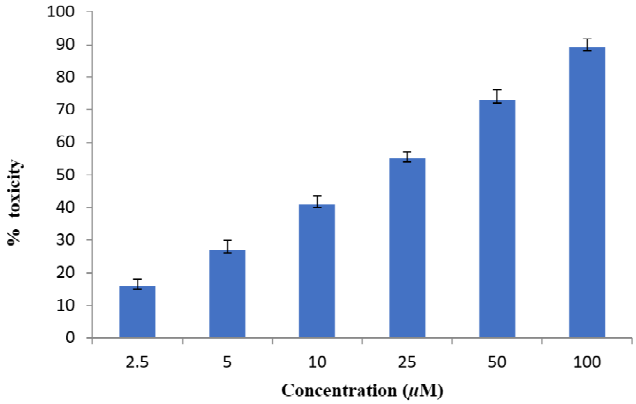

Figure 3: Cytotoxicity of DTN was assessed in L6 myocytes by MTT assay based on concentration. Values are the mean of three independent experiments done in duplicates.

2-NBDG uptake is activated by DTN

Myocytes are the key player in glucose consumption in our body. The imbalance of glucose homeostasis is one of the responsible factors for T2DM. To assess the effect of DTN treatment on glucose uptake, cells were treated with 2-NBDG, a fluorescently labelled glucose analogue, with or without DTN, for 24 h. The glucose uptake of L6 myotubes was significantly increased by DTN with an efficiency of 31.5%. The extent of this increase was comparable to that observed with metformin (100 µM: 35.2%, $P < 0.05$), the commonly used antidiabetic drug (Figure 4). Considering the glucose uptake efficacy of DTN in myotubes, it can be suggested that exploiting its ability to uptake glucose may have a major impact on systemic glycemic control. Particularly, the unique and robust ability of DTN to enhance skeletal muscle glucose uptake is of great interest, and it may be used for developing new drug targets for T2DM. Apart from these results, we suggested the possibility that DTN can activate downstream biological pathways of

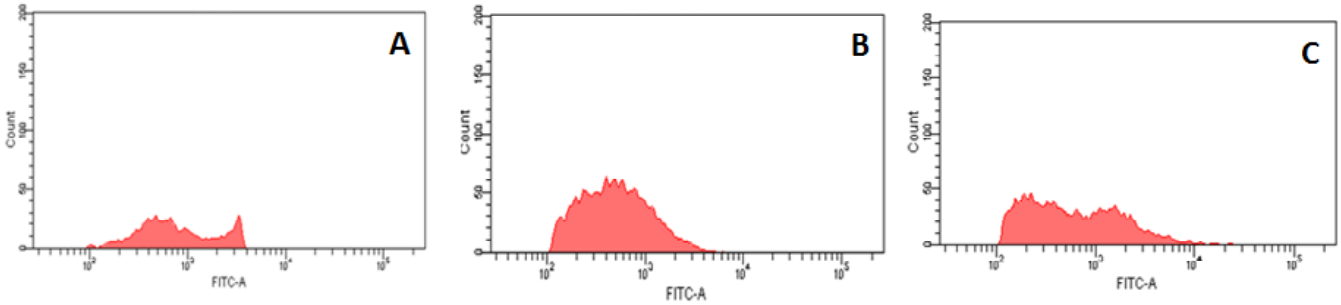

Figure 4: 2-NBDG uptake in skeletal myotubes. Flow cytometry analysis carried out using 2-NBDG in differentiated L6 myotubes by plotting cell count against FITC revealed that (A) 13.6% uptake in 2-NBDG control cells, (B) 35.3% in the positive control (100 µM metformin) treated cells and (C) 31.5% uptake cells treated with 2.5 µM DTN show% uptake in each graph

glucose uptake, thereby revealing its therapeutical potential. Moreover, the potential shown by the bioactive can further suppress the driving mechanisms behind hyperglycemic conditions.

Dactyloidin stimulated GLUT4 translocation in L6 myotubes

GLUT4 expression is exquisitely regulated in muscle and muscle GLUT4 overexpression in transgenic animals ameliorates insulin resistance associated with obesity or diabetes. In myocytes, impaired translocation of GLUT4 to the plasma membrane resulted in imbalanced glucose uptake that leads to hyperglycemia, one of the hallmark characteristics of T2DM. Therefore, DTN was evaluated for GLUT4 translocation activity in L6 myotubes. 2.5 µM DTN significantly increased the cell surface expression level of GLUT4 around two fold when compared with the positive control ($P<0.05$) (Figure 5). The standard drug, metformin (100 µM), showed a 1.38 ± 0.04-fold increase in the surface GLUT4 level in the same experimental condition. GLUT4 translocation to the plasma membrane appears to be an important cause of the enhancement of glucose uptake by DTN in L6 myotubes. The present observation is in parallel with the report that GLUT4 was expressed much more intensely than GLUT1 and GLUT3 in L6 myotubes, and a decrease in GLUT4 translocation to the plasma membranes has been implicated as a possible cause of insulin resistance, a predisposing factor of T2DM. These preliminary findings suggest that DTN may enhance glucose uptake in skeletal muscles through GLUT4 and may have therapeutic efficacy.

AMPK signalling was upregulated by DTN

To identify the mechanism underlying DTN-stimulated glucose uptake, the involvement of a non-insulin mediated pathway (AMPK) was examined. AMPK is believed to be a target for diabetic treatment based on studies demonstrating its modulation by several therapeutic agents. The preliminary studies using 2-NBDG have given evidence that DTN can stimulate glucose uptake in myotubes. To further explore the action of DTN and its downstream targets involved in stimulated glucose uptake, the involvement of AMPK signalling in DTN treated differentiated skeletal myotubes were examined by western blot analysis. Results (Figure 6) confirmed that DTN activated AMPK pathway and the activation of AMPK is considered to be the driving factor behind GLUT4 expression. The observed effect of DTN was correlated with one of the recent studies, which explain the activity of AMPK is closely correlated with glucose transport activity in rat skeletal muscle.

To the best of our knowledge, this is the first study that explored the antidiabetic activity of DTN and the mechanism by which it exerts its action in physiology. This study provides the promising

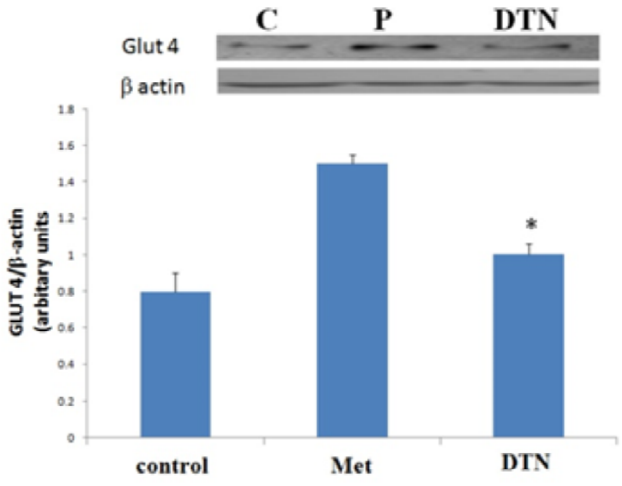

Figure 5: Western blot analysis for the expression of GLUT4 in L6 myotubes. Differentiated L6 cells were treated with DTN (2.5*m*M) and subjected to western blot analysis using β-actin as a loading control. Band intensities were expressed as a mean of three experiments±SD, '*'p 0.01.

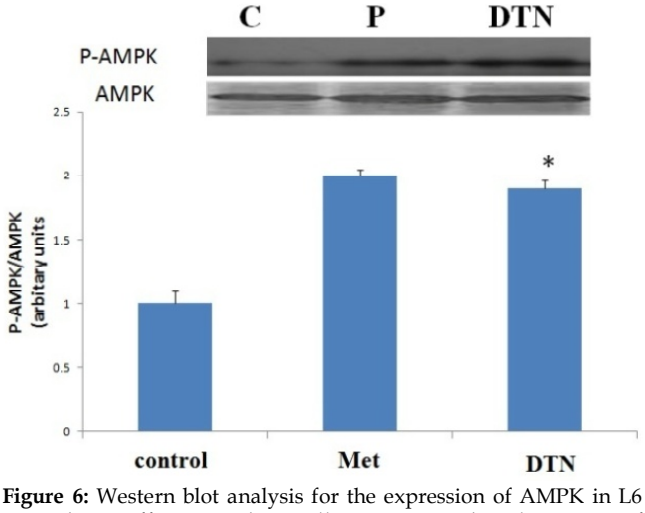

Figure 6: Western blot analysis for the expression of AMPK in L6 myotubes. Differentiated L6 cells were treated with 2.5 *m*M of DTNand subjected to western blot analysis for the expression of AMPK as detailed in the methodology section. A representative western blot using total AMPK served as a loading control. Band intensities were expressed as the mean of three experiments±SD, '*'p <0.01.

activity of DTN as an AMPK/GLUT4 activator so as to target metabolic syndrome through the downstream molecular pathways.

Collectively, the present study highlighted the potential of DTN to increase glucose uptake in skeletal muscle cells. Our data also provide novel evidence for the involvement of downstream stimulatory action of DTN through non-insulin-independent signalling cascade involving AMPK/ GLUT4 expression. The interesting aspect of DTN as an AMPK activator can pay the way for advanced studies involving *in vitro* animal models.

CONCLUSION

Phytochemical investigation of the seeds of *M. fatua* led to the isolation of diarylnonanoid dactyloidin (DTN). The antidiabetic potential of DTN was examined. DTN significantly inhibited the activity of α-glucosidase enzyme with IC_{50} value of 55.08±0.857 µM. The molecular docking studies revealed that DTN effectively binds the pocket of *N*-terminal human maltase glucoamylase (**3TOP**) with D-/G-score of -5.7. DTN enhanced the 2-NBDG uptake in L6 myotubes with 31.5 % efficiency. Further experiments confirmed that DTN stimulated the glucose uptake in skeletal muscle cells by enhancing the translocation and expression of GLUT4. Our results indicate the importance of modulating AMPK pathway for improved therapeutic approaches to T2DM and associated disorders.

REFERENCES

Adrover M, Laura MarinÞ, Sanchis P, Pauwels K, Kraan Y, Lebrun P, Vilanova B, MunÞoz F, Broersen K, Donoso J. 2014. Mechanistic insights in glycation-induced protein aggregation. *Biomacromolecules* **15**: 3449-3462.

Ajish KR, Antu KA, Riya MP, Preetharani MR, Raghu KG, Dhanya BP, Radhakrishnan KV. 2015. Studies on *á*-glucosidase, aldose reductase and glycation inhibitory properties of sesquiterpenes and flavonoids of *Zingiber zerumbet* Smith. *Nat Prod Res* **29**: 947-952.

Apostolidis E, Kwon YI, Shetty K. 2007. Inhibitory potential of herb, fruit, and fungal- enriched cheese against key enzymes linked to type 2 diabetes and hypertension. *Innov Food Sci Emerg* **8**: 46-54.

Burnette WN. 1981. Western blotting: electrophoretic transfer of proteins from sodium dodecyl sulfate-polyacrylamide gels to unmodified nitrocellulose and radiographic detection with antibody and radioiodinated protein A. *Anal Biochem* **112**: 195-203.

DeFronzo RA, Ferrannini E, Groop L, Henry RR, Herman WH, Holst JJ, Hu FB, Kahn CR, Raz I, Shulman GI, Simonson DC, Testa MA, Weiss R. 2015. Type 2 diabetes mellitus. *Nat Rev Dis Primers* **1**:1-22.

Dhanya BP, Gopalan G, Reshmitha TR, Saranya J, Sharathna P, Shibi IG, Nisha P, Radhakrishnan KV. 2017. Synthesis and *in vitro* evaluation of zerumbone pendant derivatives: potent candidates for antidiabetic and anti-proliferative activities. *New J Chem* **41**: 6960-6964.

Fajriah S, Darmawan A, Megawati, Hudiyono S, Kosela S, Hanafi M. 2017. New cytotoxic compounds from *Myristica fatua* Houtt. Leaves against MCF-7 cell lines. *Phytochem Lett* **20**: 36-39.

Gopalan G, Prabha B, Joe A, Reshmitha TR, Sherin DR, Sabu M, Manojkumar TK, Radhakrishnan KV, Nisha P. 2019. Antidiabetic properties of apiforol, a potential lead isolated from the seeds of *Musa balbisiana*. *J Sci Food Agric* **99**: 2521-2529.

Gopalan G, Dhanya BP, Saranya J, Reshmitha TR, Baiju TV, Meenu MT, Mangalam SN, Nisha P, Radhakrishnan KV. 2017. Metal free trans aziridination of zerumbone: Synthesis and biological evaluation of aziridine derivatives of zerumbone. *Eur J Org Chem* 3072-3077.

Herath HMTB, Priyadarshani AMA, Jamie J. 1998. Dactyloidin, a new diarylnonanoid from *Myristica dactyloides*. *Nat Prod Lett* **12**: 91-95.

Huang S, Czech MP, 2007. The Glut4 glucose transporter. Cell Metab **5**: 237 -252.

Jedsadayanmata A. 2005. *In vitro* antiglycation activity of arbutin. *J Naresun Univ* **13**: 35-41.

Kim Y, Park CW. 2016. Adenosine monophosphate–activated protein kinase in diabetic nephropathy. *Kidney Res Clin Pract* **35**: 69-77.

Megawati, Darmawan A. 2017. Resorcinol compounds isolated from the bark of *Myristica fatua* Houtt. *Indonesian J Pharm* **28**: 82-90.

Mosmann T. 1983. Rapid colorimetric assay for cellular growth and survival: application to proliferation and cytotoxicity assays. *J Immunol Meth* **65**: 55-63.

Pandey R, Mahar R, Hasanain M, Shukla SK, Sarkar J, Rameshkumar KB, Kumar B, 2016. Rapid screening and quantitative determination of bioactive compounds from fruit extracts of Myristica species and they're *in vitro* antiproliferative activity. *Food Chem* **211**: 483-493.

Prabha B, Neethu S, Lekshmy Krishnan S, Sherin DR, Madhukrishnan M, Ananthakrishnan R, Rameshkumar KB, Manojkumar TK, Jayamurthy P, Radhakrishnan KV. 2018. Antidiabetic potential of phytochemicals isolated from the stem bark of *Myristica fatua*Houtt. var. Magnifica (Bedd.) Sinclair. *Bioorg Med Chem* **26**: 3461-3467.

Prabha B, Sini S, Sherin DR, Neethu S, Rameshkumar KB, Manojkumar TK, Jayamurthy P, Radhakrishnan KV. 2019. Promalabaricone B from *Myristica fatua*Houtt. var. Magnifica(Bedd.) Sinclair seeds demonstrate antidiabetic potential by inhibiting carbohydrate hydrolyzing enzymes protein glycation and modulating glucose uptake via the activation of AMPK in L6 myotubes. *Nat Prod Res*https://doi.org/10.1080/14786419.1607852.

Prabhakar PK, Doble M. 2011. Interaction of cinnamic acid derivatives with commercial hypoglycemic drugs on 2-deoxyglucose uptake in 3T3-L1 adipocytes. *J Agric Food Chem* **59**: 9835-9844.

Ren LM, Qin XH, Cao XF, Wang LL, Bai F, Bai G, Shen Y. 2011. Structural insight into substrate specificity of human intestinal maltase-glucoamylase. *Prot Cell* **2**: 827-836.

Sasikumar P, Lekshmy K, Sini S, Prabha B, Kumar NA, Sivan VV, Jithin MM, Jayamurthy P, Shibi IG, Radhakrishnan KV. 2019. Isolation and characterization of resveratrol oligomers from the stem bark of *Hopea ponga* (Dennst.) Mabb. and their antidiabetic effect by modulation of digestive enzymes, protein glycation and glucose uptake in L6 myocytes. *J Ethnopharmacol* **236**: 196-204.

Sasikumar P, Prabha B, Reshmitha TR, Sheeba V, Pradeep AK, Rohit KR, Dhanya BP, Sivan VV, Jithin MM, Anil Kumar N, Shibi IG, Nisha P, Radhakrishnan KV. 2016. Comparison of antidiabetic potential of (+) and (-)-Hopeaphenol, a pair of enantiomers isolated from *Ampelocissus indica* (L.) and *Vateria indica* Linn, with respect to inhibition of digestive enzymes and induction of glucose uptake in L6 myotubes. *RSC Adv* **6**: 77075-77082.

Sasikumar P, Sharathna P, Prabha B, Varughese S, Kumar NA, Sivan VV, Sherin DR, Suresh E, Manojkumar TK, Radhakrishnan KV. 2018. Dihydro-β-agarofuran sesquiterpenoids from the seeds of *Celastrus paniculatus* Willd. and their α- glucosidase inhibitory activity. *Phytochem Lett* **26**: 1-8.

Sim L, Quezada-Calvillo R, Sterchi EE, Nichols BL, Rose DR. 2008. Human intestinal maltase-glucoamylase: crystal structure of the N-terminal catalytic subunit and basis of inhibition and substrate specificity. *J Mol Biol* **375**: 782-792.

Somwar R , Sweeney G, Ramlal T, Klip A. 1998. Stimulation of glucose and amino acid transport and activation of the insulin signalling pathways by insulin lisproin L6 skeletal muscle cells. *Clin Ther* **20**: 125-140.

Tamrakar AK, Jaiswal N, Yadav PP, Maurya R, Srivastava AK. 2011. Pongamol from *Pongamia pinnata* stimulates glucose uptake by increasing surface GLUT4 levels in skeletal muscle cells. *Mol Cell Endocrinol* **339**: 98-104.

Trapero A, Llebaria A. 2012. A prospect for pyrrolidine iminosugars as antidiabetic β-glucosidase inhibitors. *J Med Chem* **55**: 10345-10346.

Victor JN, John RS. 2006. Drug-related hepatotoxicity. *N Engl J Med* **354**: 731-739.

Williams LK, Li C, Withers SG, Brayer GD. 2012. Order and disorder: differential structural impacts of myricetin and ethyl caffeate on human amylase, an antidiabetic target. *J Med Chem* **55**: 10177-10186.

Xio Z, Storms R , Tsang A. 2006. A quantitative starch–iodine method for measuring alpha-amylase and glucoamylase activities. *Anal Biochem* **351**: 146-148.